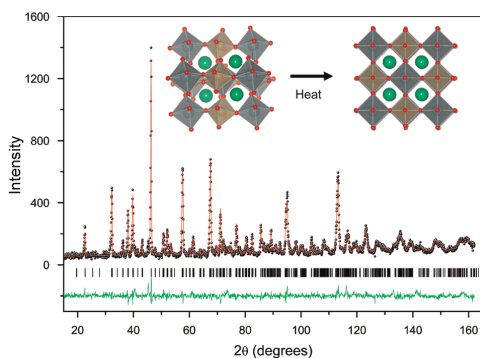


Abstracted/indexed in BioEngineering Abstracts, Chemical Abstracts, Coal Abstracts, Current Contents/Physics, Chemical, & Earth Sciences, Engineering Index, Research Alert, SCISEARCH, Science Abstracts, and Science Citation Index. Also covered in the abstract and citation database SCOPUS[®]. Full text available on ScienceDirect[®].

Regular Articles

Structural studies of the disorder and phase transitions in the double perovskite Sr₂YTaO₆

Qingdi Zhou, Brendan J. Kennedy and Maxim Avdeev
Page 1741

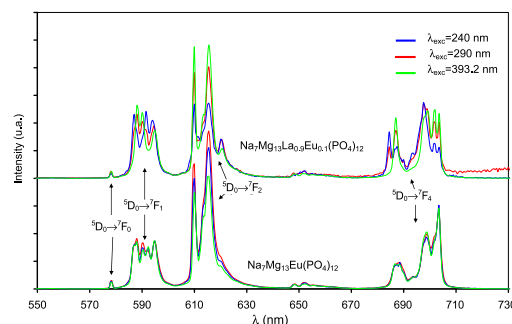


Sr₂YTaO₆ undergoes a sequence of phase transitions upon heating associated with the removal of the tilting of the octahedral. The number of defects in the structure is sensitive to the preparative conditions.

Regular Articles—Continued

Synthesis, crystal structure and optical investigation of the new phosphates: Na₇Mg₁₃Ln(PO₄)₁₂ (Ln = La, Eu)

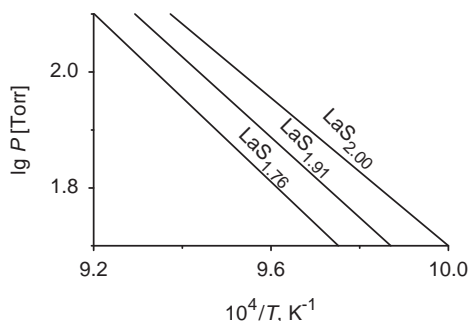
Hasna Jerbi, Mourad Hidouri, Benoit Glorieux, Jacques Darriet, Alain Garcia, Véronique Jubera and Mongi Ben Amara
Page 1752



Emission spectra of Na₇Mg₁₃Eu(PO₄)₁₂ and Na₇Mg₁₃La_{0.9}Eu_{0.1}(PO₄)₁₂ compounds for λ_{exc} = 240, 290 and 393.2 nm.

The La₂S₃–LaS₂ system: Thermodynamic and kinetic study

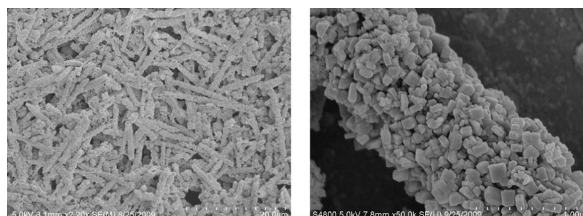
I.G. Vasilyeva and R.E. Nikolaev
Page 1747



The p - T stability fields for La-polysulfides in the concentration range between LaS₂ and La₂S₃.

Polymer-directed synthesis and magnetic property of nanoparticles-assembled BiFeO₃ microrods

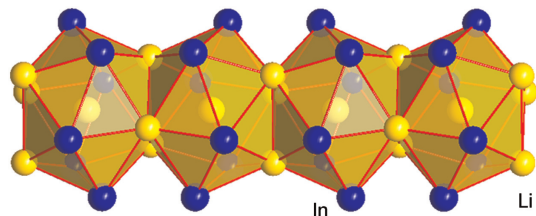
Lei Zhang, Xiao-Feng Cao, Ying-Li Ma, Xue-Tai Chen and Zi-Ling Xue
Page 1761



Nanoparticles-assembled BiFeO₃ microrods were successfully prepared via a polymer-directed solvothermal route and characterized by XRD, EDS, FT-IR, ICP-AES and SEM.

Intermetallic and metal-rich phases in the system Li–Ba–In–N

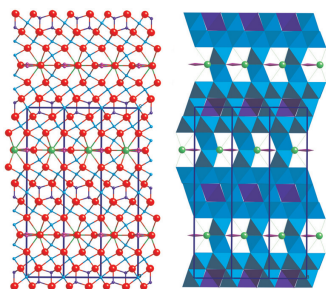
Volodymyr Smetana, Grigori V. Vajenine, Lorenz Kienle, Viola Duppel and Arndt Simon
Page 1767



One-dimensional chain of face-sharing centered icosahedra in $\text{BaLi}_{2.1}\text{In}_{1.9}$.

Characterizing CA_2 and CA_6 using ELNES

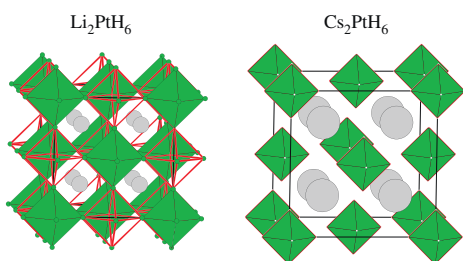
A. Altay, C.B. Carter, P. Rulis, W.-Y. Ching, I. Arslan and M.A. Gülgün
Page 1776



Projection of the CA_2 structure viewed in the $[010]$ direction. Green atoms represent the Ca^{2+} ions and blue atoms represent the Al^{3+} ions. Two unit cells are outlined.

Synthesis of Li_2PtH_6 using high pressure: Completion of the homologous series A_2PtH_6 ($A = \text{alkali metal}$)

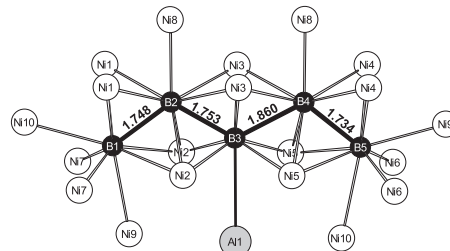
Kati Puhakainen, Emil Stoyanov, Michael J. Evans, Kurt Leinenweber and Ulrich Häussermann
Page 1785



Li_2PtH_6 , the missing start member of the complex metal hydride series A_2PtH_6 ($A = \text{alkali metal}$) has been prepared by high pressure hydrogenation. In contrast to the heavier homologues, PtH_6^{2-} octahedral units in Li_2PtH_6 are not well separated and H atoms form a substructure closely corresponding to that of O atoms in cubic perovskite.

Synthesis and crystal structures of the new metal-rich ternary borides $\text{Ni}_{12}\text{AlB}_8$, $\text{Ni}_{12}\text{GaB}_8$ and $\text{Ni}_{10.6}\text{Ga}_{0.4}\text{B}_6$ —examples for the first B_5 zig-zag chain fragment

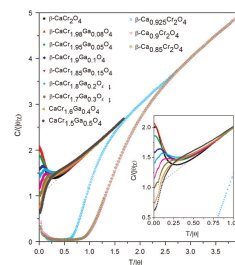
Martin Ade, Dominik Koztott and Harald Hillebrecht
Page 1790



Pentameric B_5 -units are longest fragments of a B–B zig-zag chain ever characterized in a boride. They are found in the structures of $\text{Ni}_{12}\text{AlB}_8$ and $\text{Ni}_{12}\text{GaB}_8$. The compounds are formed on annealing boron-rich τ -borides like $\text{Ni}_{20}\text{AlB}_{14}$.

Divergent effects of static disorder and hole doping in geometrically frustrated $\beta\text{-CaCr}_2\text{O}_4$

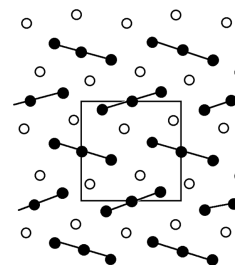
S.E. Dutton, C.L. Broholm and R.J. Cava
Page 1798



Scaled plot of the temperature dependence of the inverse susceptibility for $\beta\text{-CaCr}_{2-2x}\text{Ga}_{2x}\text{O}_4$ (closed symbols) and $\beta\text{-Ca}_{1-y}\text{Cr}_2\text{O}_4$ (open symbols). Data sets depicted in the same color contain equivalent amounts of Cr^{3+} .

Magnetic properties of linear trimers in fluoride analogs of tetragonal tungsten bronze

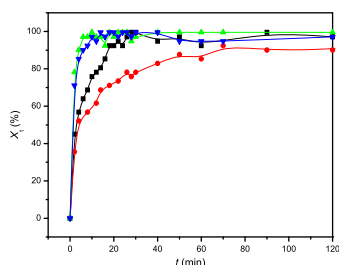
Yaw-Shun Hong, William O.J. Boo and Daniell L. Mattern
Page 1805



Five fluoride analogs of Tetragonal Tungsten Bronze (KZnTiF_6 , KZnVF_6 , KVScF_6 , KCrScF_6 , and KMnScF_6) underwent $\text{M}^{2+}\text{--M}^{3+}$ ionic ordering below 100 K, providing linear trinuclear complexes of their respective paramagnetic ions.

Synthesis and release behavior of composites of camptothecin and layered double hydroxide

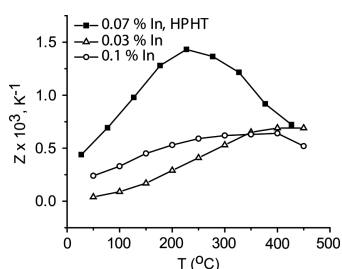
Lun Dong, Li Yan, Wan-Guo Hou and Shao-Jie Liu
Page 1811



A simple method, reconstruction of calcinated LDHs in an organic-water medium containing drug, was developed to intercalate non-ionic and poorly water-soluble camptothecin into the gallery of LDHs.

Thermoelectric properties of HPHT sintered In-doped $\text{Pb}_{0.5}\text{Sn}_{0.5}\text{Te}$

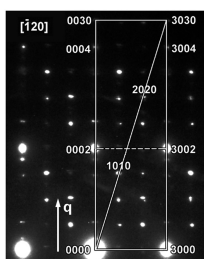
Yongkwan Dong, Abds-Sami Malik and Francis J. DiSalvo
Page 1817



A twofold improvement in thermoelectric figure of merit (ZT) is achieved for HPHT sintered In-doped $\text{Pb}_{0.5}\text{Sn}_{0.5}\text{Te}$, when compared to the conventionally sintered materials of similar composition reported in the literature.

The local structure and composition of $\text{Ba}_4\text{Nb}_2\text{O}_9$ -based oxycarbonates

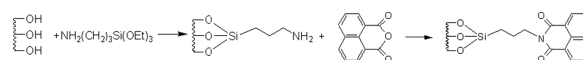
Jana Bezjak, Artem M. Abakumov, Aleksander Rečnik, Marjeta Maček Kržmanc, Boštjan Jančar and Danilo Suvorov
Page 1823



The composition and the local crystal structure of generally known $\alpha\text{-Ba}_4\text{Nb}_2\text{O}_9$ was studied. The compound is hydrated oxycarbonate with the composition of $\text{Ba}_4\text{Nb}_2\text{O}_{8.8}(\text{CO}_3)_{0.2} \cdot 0.1 \text{H}_2\text{O}$. It has a composite incommensurately modulated structure consisting of two mutually interacting subsystems, i.e., $[\text{Ba}]_\infty$ and the $[(\text{Nb}, \square)\text{O}_3]_\infty$ subsystem.

Post-treatment and characterization of novel luminescent hybrid bimodal mesoporous silicas

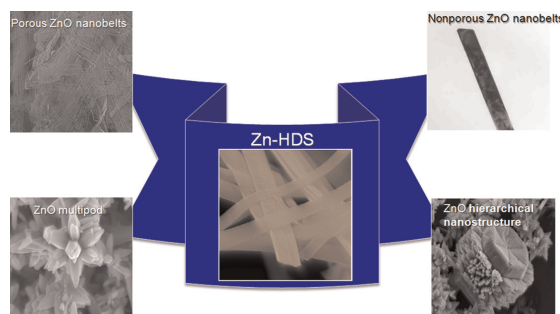
Yuzhen Li, Jihong Sun, Xia Wu, Li Lin and Lin Gao
Page 1829



A novel luminescent hybrid bimodal mesoporous silica was synthesized via modification and then grafting with 1, 8-Naphthalic anhydride, which would be strong potential application in the photoluminescent fields.

Synthesis of porous and nonporous ZnO nanobelt, multipod, and hierarchical nanostructure from Zn-HDS

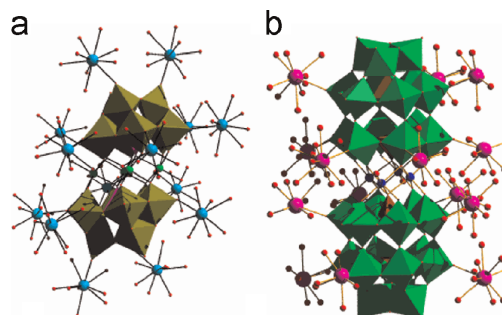
Eue-Soon Jang, Jung-Hee Won, Young-Woon Kim, Zhen Cheng and Jin-Ho Choy
Page 1835



Porous and nonporous ZnO nanobelts, multipod, and hierarchical nanostructure were successfully synthesized from Zn based hydroxyl double salts by hydrothermal reaction.

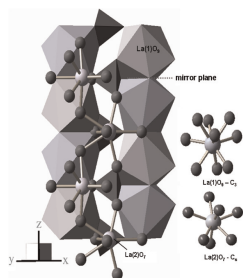
Two 3D networks based on sandwich-type polyoxometalate units linked by Sr-O clusters: Synthesis, structure, and magnetic property

Yang Yu, Bai-Bin Zhou, Kai Yu and Yu-Nan Zhang
Page 1841



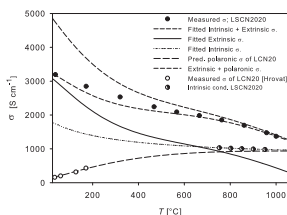
Two compounds based on Keggin(a) and Wells-Dawson(b) polyoxometalates modified by 14 Sr-O clusters.

Eu³⁺ luminescence in La₅Si₂BO₁₃ with apatite related structure and magnetic studies in Ln₅Si₂BO₁₃ (Ln = Gd, Dy)
 S. Asiri Naidu, U.V. Varadaraju and B. Raveau
 Page 1847



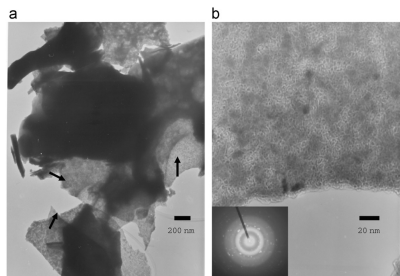
In La₅Si₂BO₁₃, the La(1)O₉ polyhedra share faces, the La(2)O₇ polyhedra are connected through corners and La(2)O₇ and La(1)O₉ polyhedra are connected to each other by edge sharing along z'-axis.

Defect structure, electronic conductivity and expansion of properties of (La_{1-x}Sr_x)₅Co_{1-y}Ni_yO_{3-δ}
 Per Hjalmarsen, Martin Sogaard and Mogens Mogensen
 Page 1853



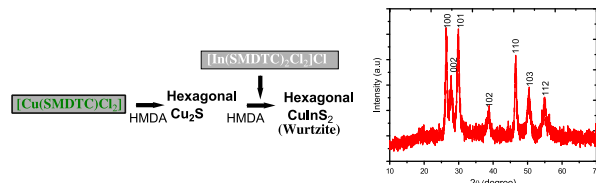
Electronic conductivity as a function of temperature for (La_{0.8}Sr_{0.2})_{0.99}Co_{0.8}Ni_{0.2}O_{3-δ}. A model with metallic like conductivity for the extrinsic p-type charge carrier (due to Sr substitution) and small polaron conductivity for intrinsic charge carriers (due to Co spin transitions) was found to best describe the total conductivity.

Magneto-thermal and dielectric properties of biferroic YCrO₃ prepared by combustion synthesis
 A. Durán, A.M. Arévalo-López, E. Castillo-Martínez, M. García-Guaderrama, E. Moran, M.P. Cruz, F. Fernández and M.A. Alario-Franco
 Page 1863



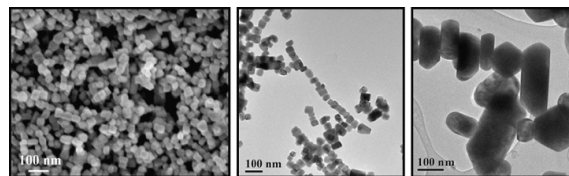
Combustion method: An alternative route for synthesized a new family of multiferroics. Amorphous agglomerates of nano-sized particles of YCrO₃ compounds.

Facile synthesis of nanocrystalline wurtzite Cu–In–S by amine-assisted decomposition of precursors
 Pulakesh Bera and Sang Il Seok
 Page 1872



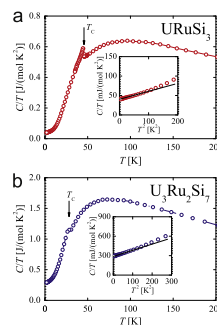
Phase-pure ternary wurtzite Cu–In–S nanocrystals have been synthesized by a simple amine-assisted decomposition of mixed precursor complexes derived from S-methyl dithiocarbazate (SMDTC) at a relatively low temperature.

Shape-controlled solvothermal synthesis of bismuth subcarbonate nanomaterials
 Gang Cheng, Hanmin Yang, Kaifeng Rong, Zhong Lu, Xianglin Yu and Rong Chen
 Page 1878



Different bismuth subcarbonate ((BiO)₂CO₃) nanostructures were successfully synthesized by a simple solvothermal method. It was found that the solvents and precursors have an influence on the morphologies of (BiO)₂CO₃ nanostructures.

Crystal structure and physical properties of the novel ternary intermetallics URuSi_{3-x} and U₃Ru₂Si₇
 M. Pasturel, A.P. Pikul, M. Potel, T. Roisnel, O. Tougait, H. Noël and D. Kaczorowski
 Page 1884

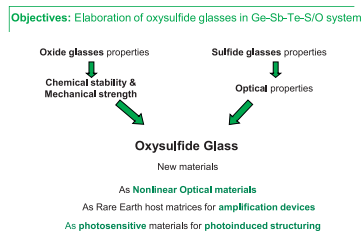


Thermal dependence of the specific heat of the novel intermetallics URuSi₃ and U₃Ru₂Si₇. The arrows mark temperatures of ferro- or ferrimagnetic phase transitions.

Processing and characterization of new oxy-sulfo-telluride glasses in the Ge-Sb-Te-S-O system

C. Smith, J. Jackson, L. Petit, C. Rivero-Baleine and K. Richardson

Page 1891

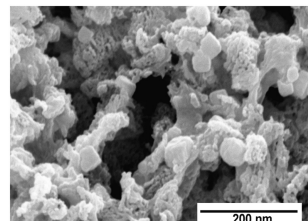


In this paper, we discuss our most recent findings on the processing and characterization of new ChG glasses prepared with small levels of Te, melted either with TeO_2 or Sb_2O_3 powders. We explain how these new oxy-sulfo-telluride glasses are prepared and we correlate the physical, thermal and optical properties of the investigated glasses to the structure changes induced by the addition of oxygen in the Ge-Sb-S-Te glass network.

Chemical synthesis of mesoporous CuO from a single precursor: Structural, optical and electrical properties

Swarup Kumar Maji, Nillohit Mukherjee, Anup Mondal, Bibhotosh Adhikary and Basudeb Karmakar

Page 1900



FESEM image of the mesoporous CuO prepared from $\text{Cu}(\text{OOCPh})_2$ Lut_2 complex.

Author inquiries

For inquiries relating to the submission of articles (including electronic submission where available) please visit this journal's homepage at <http://www.elsevier.com/locate/jssc>. You can track accepted articles at <http://www.elsevier.com/trackarticle> and set up e-mail alerts to inform you of when an article's status has changed. Also accessible from here is information on copyright, frequently asked questions and more. Contact details for questions arising after acceptance of an article, especially those relating to proofs, will be provided by the publisher.

Language services. Authors who require information about language editing and copyediting services pre- and post-submission please visit <http://www.elsevier.com/locate/languagepolishing> or our customer support site at <http://epsupport.elsevier.com>. Please note Elsevier neither endorses nor takes responsibility for any products, goods or services offered by outside vendors through our services or in any advertising. For more information please refer to our Terms & Conditions <http://www.elsevier.com/termsandconditions>

For a full and complete Guide for Authors, please go to: <http://www.elsevier.com/locate/jssc>

Journal of Solid State Chemistry has no page charges.